Published in final edited form as:
FEBS Lett. 2006 October 30; 580(25): 5959–5964.

Structure–function studies of the G-domain from human gem, a novel small G-protein

Yarden Opatowsky[c], **Yehezkel Sasson**[c], **Isabella Shaked**[c], **Yvona Ward**[a], **Orna Chomsky-Hecht**[c], **Yael Litvak**[b], **Zvi Selinger**[b], **Kathleen Kelly**[a], and **Joel A. Hirsch**[c,*]

a *Cell and Cancer Biology Branch, Center for Cancer Research, NCI, NIH, Bethesda, MD, USA*

b *Department of Biological Chemistry, Institute of Life Sciences, The Hebrew University, Jerusalem, Israel*

c *Department of Biochemistry, Faculty of Life Sciences, Daniella Rich Institute for Structural Biology, Tel Aviv University, Ramat Aviv 69978, Israel*

Abstract

Gem, a member of the Rad, Gem/Kir subfamily of small G-proteins, has unique sequence features. We report here the crystallographic structure determination of the Gem G-domain in complex with nucleotide to 2.4 Å resolution. Although the basic Ras protein fold is maintained, the Gem switch regions emphatically differ from the Ras paradigm. Our ensuing biochemical characterization indicates that Gem G-domain markedly prefers GDP over GTP. Two known functions of Gem are distinctly affected by spatially separated clusters of mutations.

Keywords

G-protein; Crystallography; Nucleotide; Calcium channel; Cytoskeleton

1. Introduction

The Ras superfamily of small G-proteins is both large and diverse. Several subfamilies have been categorized including the Rad,Gem/Kir (RGK) subfamily. This group now includes four members: Rad, Gem, Rem, and Rem2. These molecules were initially identified independently as transcriptionally regulated G-proteins [1–3] but their physiological function has remained challenging to define.

Within the Ras superfamily, the RGK subfamily is structurally distinguished by unique N and C-terminal sequence motifs, and within the G domain, by changes in normally highly conserved amino acids that are involved in nucleotide binding and GTP hydrolysis. Significant differences in Gem relative to Ras include the absence of an equivalent to T35, which stabilizes Mg-GDP/GTP binding, and a loss of the G3 motif, DXXG, which contributes to nucleotide binding and GTPase catalysis. To date, the biochemical functions identified for the N and C terminal extensions include binding 14-3-3 and binding Ca^{2+}/calmodulin (CaM) [4]. These unique features raise questions regarding the subfamily's enzymatic activity, directly related to its function as a molecular switch.

Recent cell biologic and biochemical characterization of different subfamily members has forged progress in revealing functional information (reviewed in [4]). In particular, two independent effector pathways have been defined for Gem, namely regulation of voltage-

*Corresponding author. Fax: +972 3 6407931., E-mail address: jhirsch@post.tau.ac.il (J.A. Hirsch).

NIH-PA Author Manuscript

NIH-PA Author Manuscript

dependent calcium channel (VDCC) signaling and cytoskeletal organization as mediated through ROK (also known as ROCK/Rhokinase). In order to better understand the action of these molecules, we have initiated a structure–function study of human Gem. We chose first to characterize the three-dimensional structure and biochemical activity of Gem's G-domain as a starting point, thereby providing essential basic biochemical information. Thus, we report here a 2.4 Å crystallographic structural determination and biochemical studies. On the basis of this data, we have also engineered several mutations that have been tested in a cell-based functional context.

2. Materials and methods

Subcloning, expression, purification, crystallization, data collection, and structure determination are described in detail in supplementary material available online. Gem G-domain was bacterially overexpressed, purified with the help of a removable histidine tag, and subsequently crystallized. Structure determination was by single anomalous diffraction using a selenomethionine derivative.

The reversed-phase HPLC nucleotide identification assay was performed as described [5]. GTP hydrolysis assays were performed as described [6]. Gem-dependent ROK-mediated cytoskeletal rearrangements were assayed using transient co-transfection of N1E-115 neuroblastoma cells as described [7]. Co-immunoprecipitation of Gem and Flag-tagged CaVβ2A or 1B was performed using lysates from transiently transfected COS7 cells precipitated with anti-FLAG antibodies and blotted with anti-Gem polyclonal antibodies.

3. Results and discussion

Using our purified Gem G-domain prepared with a non-hydrolyzable GTP analog, diffracting crystals were obtained. Data measured on a home X-ray source enabled molecular replacement calculations. The solution gave reasonable electron density maps in regions of the central β-sheet but poor density in other locations. Rounds of model building improved the maps and indicated regions of significant divergence from the starting model. In order to validate our structure and obtain independent phasing, selenomethionine protein was prepared and a single wavelength anomalous diffraction experiment performed. The experimentally phased map clearly confirmed and completed regions of our model (Table 1). Moreover, it unambiguously confirmed that in place of the expected GTP analog, GDP was found. This finding raised questions regarding the conditions of nucleotide exchange, binding and hydrolysis for the Gem G-domain. Further biochemical characterization described below leads us to conclude that our attempt to load Gem G-domain with β,γ-imido-GTP (GMPPNP) in preparation for crystallization was not successful.

The refined structure comprises residues 72–243, with breaks at residues 99–102 and 137–138. The G-domain takes the canonical Ras fold with the central β-sheet of six strands and five surrounding α-helices. A superposition with Ras-GDP indicates a RMS deviation of 1.1 Å for 146 Cα atoms. There are notable differences between the Ras family of structures and Gem. The most outstanding structural variation is the region of switch I (Fig. 1A). In contrast to Ras, whose switch I covers the bound nucleotide, in Gem the loop emerging from α1 helix changes trajectory and runs closer to the surface of the protein, completely leaving the nucleotide pocket exposed. The ''phosphate binding'' loop then ''returns'' to the canonical fold with a shortened (versus Ras) β2 strand. Inspection of the structure based sequence alignment (Fig. 2) shows that this sequence region linking α1 and β2, which includes G-1, has no similarity with Ras. Moreover, even within the RGK family there is little sequence conservation with varying lengths for this loop, Gem having the longest.

Another important but subtler difference in the G-domain fold between the prototypical Ras and Gem is found in the end of β3 and the loop linking it with α2. This sequence region comprises switch II. Gem's fold only approximates the Ras trajectory, is further from the bound nucleotide, its α2 takes a somewhat different orientation and the packing between the extended chain emerging from β3 and α2 appears quite robust. A molecular lynchpin is created by the stacking of W133 and H143 (from α2), seeming to rigidify this structural module (Fig. 1C). W133 is perfectly conserved among RGK family members. In Ras, this switch II is known to encompass the γ-phosphate of the nucleotide and to be quite flexible. Sequence comparisons for this region indicate a remarkable divergence compared to Ras. The conserved G3 motif, DXXG, in Ras is replaced by DXWEX at the comparable position in RGK proteins.

Many nucleotide interactions between the G-domains and the bound nucleotide are similar (Fig. 1B and D). However, there are pointed exceptions. For example, N135, equivalent to Ras Q61, a residue critical for GTP hydrolysis as it stablilizes the nucleophilic water (see [8] for a summary of G-protein catalytic mechanisms), would be far from the γ-phosphate and its bridging O unless significant movement was induced. Such flexibility seems unlikely given the conformation of Gem's switch II. Nevertheless, Q84 may be positioned to replace it since it is within 4 Å of the Mg^{2+} coordination shell . This residue superimposes well with Ras G12. Other important interactions are missing in Gem. In Ras, K147 and F28 interact with the guanine base by van der Waals interactions. In Gem, these are absent. Moreover, the equivalent of catalytically important Ras T35 is not positioned due to the change in switch I conformation. One interaction that does appear in Gem and is reminiscent of G_α is T90 hydrogen-bonding with the nucleotide α-phosphate. Nonetheless, Gem maintains fewer interactions with nucleotide in comparison to Ras.

A significant structural difference between Gem and the Ras family lies in the burial of the nucleotide. This difference is readily apparent from Fig. 1D. About 90 out of 600 $Å^2$ from the ligand is more solvent accessible in the Gem structure. Furthermore, the apparent electrostatic potential of Gem appears to be significantly more electronegative apposite the nucleotide phosphates and in particular where a γ-phosphate might fit than Ras (Fig. 1D). The substitution of E134 for glycine clearly causes the increased electronegativity (Fig. 1B). Together, these features underscore the uniqueness of Gem's G-domain. In contrast to Ras, comparison of our Gem G-domain-GDP structure with the just published Rad G-domain-GDP structure [9] reveals that the superposed structures align well (0.6 Å for 144 *C*α atoms). The notable structural features described above are generally shared, although switch I is not seen at all in Rad while switch II is also more disordered than in the Gem structure (supplemental Fig. 1).

Our structure solution provoked several questions: first, does Gem bind GTP?; second, if so, does it induce a conformational switch?; and third, if Gem indeed binds GTP, can it hydrolyze it? In our attempt to answer the fundamental question, i.e. that of GTP binding, we performed a comprehensive screen for conditions to empty the G-domain of nucleotide. Using an established reversed-phase HPLC assay to identify the nucleotide content of Gem, we defined conditions to remove the Mg^{2+}:GDP. Protein was incubated at RT with immobilized alkaline phosphatase in the absence of Mg^{2+} (having been removed previously by desalting) and in the presence of the non-hydrolyzable GMPPNP [10]. The nucleotide state was examined by HPLC after desalting to remove the excess GMPPNP and alkaline phosphatase reaction products. After 2 h, no nucleotide was detectable. This empty Gem G-domain was then incubated with 10 mM Mg^{2+} and two-fold molar excess of GDP, GTP, or GMPPNP in independent experiments, run over a gel filtration column equilibrated with Mg^{2+} to remove unbound nucleotide and then analyzed for nucleotide bound. Wild type (WT) Gem and three substitution mutants in residues surrounding the nucleotide binding site (S89N, E134A and Q84A) were assayed (Fig. 3A). GDP was found bound to Gem while no detectable trace was found for GTP or GMPPNP. Thus, GDP could be exchanged i.e. loaded and unloaded onto Gem whereas GTP or its analog could not. This finding argues for a very marked preference of Gem for GDP versus GTP, with stable binding and slow off-rates. E134A and Q84A behaved similarly to WT, while S89N did not bind any nucleotide. This is in contrast to the homologous Ras S17N mutant that maintains a GDP bound state and acts as a dominant negative as a result of non-productive complexes with upstream activators. The GDP preference of WT Gem is entirely consistent with our crystallographic results that despite protocols to exchange the nucleotide and an extended multi-day purification, GDP was found homogeneously bound to the protein. Perhaps in a similar vein, Rem2, a RGK member, has a GDP dissociation rate markedly slower than for GTP [11]. In contrast, we have recently expressed and purified the Rad G-domain under the same conditions as for Gem. Rad was found to have a significant GTP-bound fraction (data not shown). This finding may be related to a more mobile switch II for Rad since, for example, the equivalent of E134 and N135 are not visualized in that structure but further structural studies will be necessary to test this possibility.

In parallel with our characterization of Gem's nucleotide binding, we examined the ability of Gem to hydrolyze GTP. In enzymological assays measuring single turnover or steady-state γ-phosphate release, our isolated recombinant protein, whether loaded with GDP or empty of nucleotide produced no evidence of GTPase activity (Fig. 3B and C). The assays were executed under standard conditions for small G-proteins wherein Ras was utilized as the positive control. Further, we tested not only the Gem G-domain but the bacterially expressed full length protein alone and with Ca^{2+}-CaM (supplemental Fig. 2). Neither of these forms showed hydrolytic activity.

We next asked what might be the functional consequences of perturbing six different residues that based on the structure seem to play unique roles in Gem function. Our functional test was dual-pronged: one, we examined binding of the full length Gem to the VDCC β subunit as assessed by co-immunoprecipitation in transfected cells and, two, we probed cytoskeletal reorganization, mediated by ROK with a cell morphology assay. Four mutations (S89N, T90A, E134A, N135A) surrounding the nucleotide binding region, which have been described above, were engineered. Q84, located in proximity of the GDP terminal phosphate was mutated to alanine. An additional mutation (D105K), designed to possibly lock switch I's open conformation by formation of a novel salt bridge, was also tested. The results, summarized in Fig. 4, show that T90A mutant had reduced functional activity in both assays, but the S89N, E134A, N135A, and D105K mutants had differential effects relative to the two functional assays. The indicated mutants coprecipitated less with CaVβ2a or CaVβ1b as compared to WT Gem, while maintaining ROK-dependent activity. These data are consistent with and add to previous observations suggesting that nucleotide binding is necessary for Gem inhibition of VDCC activity but is not as stringently required for inhibition of ROK activity [12]. By contrast, Q84A interacted normally with CaVβ2a and CaVβ1b but was inactive in the ROK-dependent assay. Because S89N does not bind nucleotide, yet maintains ROK-mediated cytoskeletal effects, these data demonstrate that Gem-dependent ROK function is independent of nucleotide binding. In summary, several Gem loss of function mutants segregate with respect to Gem-dependent VDCC and ROK activities.

In conclusion, the Gem G-domain structure displays dramatically divergent structural features, particularly in the two switch regions. The protein also significantly prefers binding GDP, an unusual characteristic for G-proteins. This preference may be based in part on the electrostatics of the structure. It remains possible that the Gem N and C-terminal extensions provide exchange functionality for binding GTP, although we have no evidence for this. Perhaps other proteins might provide this activity. Reports describing functional differences dependent on nucleotide state were not performed with purified components [13]. Further investigation of Gem's structure–function correlates promises to provide insight into this intriguing G-protein's molecular mechanism.

Acknowledgements

Thanks go to the staff of ID14-4 (ESRF, France) for assistance with diffraction experiments. We thank Doug Andres for generously sharing Cavβ expression constructs. Preliminary studies were supported by a grant from the US–Israel Binational Science Foundation (JAH, KK). Continuing work has been funded by a grant to JAH from the Israel Cancer Research Fund and by NIH grant EY 03529 to ZS.

References

1. Maguire J, Santoro T, Jensen P, Siebenlist U, Yewdell J, Kelly K. Gem: an induced, immediate early protein belonging to the Ras family. Science 1994;265:241–244. [PubMed: 7912851]
2. Cohen L, et al. Transcriptional activation of a ras-like gene (kir) by oncogenic tyrosine kinases. Proc Natl Acad Sci USA 1994;91:12448–12452. [PubMed: 7809057]
3. Reynet C, Kahn CR. Rad: a member of the Ras family overexpressed in muscle of type II diabetic humans. Science 1993;262:1441–1444. [PubMed: 8248782]
4. Kelly K. The RGK family: a regulatory tail of small GTP-binding proteins. Trends Cell Biol 2005;15:640–643. [PubMed: 16242932]
5. Tucker J, Sczakiel G, Feuerstein J, John J, Goody RS, Wittinghofer A. Expression of p21 proteins in *Escherichia coli* and stereochemistry of the nucleotide-binding site. EMBO J 1986;5:1351–1358. [PubMed: 3015600]
6. Brinkmann T, Daumke O, Herbrand U, Kuhlmann D, Stege P, Ahmadian MR, Wittinghofer A. Rap-specific GTPase activating protein follows an alternative mechanism. J Biol Chem 2002;277:12525–12531. [PubMed: 11812780]
7. Leone A, Mitsiades N, Ward Y, Spinelli B, Poulaki V, Tsokos M, Kelly K. The Gem GTP-binding protein promotes morphological differentiation in neuroblastoma. Oncogene 2001;20:3217–3225. [PubMed: 11423971]
8. Scrima A, Wittinghofer A. Dimerisation-dependent GTPase reaction of MnmE: how potassium acts as GTPase-activating element. EMBO J 2006;25:2940–2951. [PubMed: 16763562]
9. Yanuar A, Sakurai S, Kitano K, Hakoshima T. Crystal structure of human Rad GTPase of the RGK-family. Genes Cell 2006;11:961–968.
10. John J, Sohmen R, Feuerstein J, Linke R, Wittinghofer A, Goody RS. Kinetics of interaction of nucleotides with nucleotide-free H-ras p21. Biochemistry 1990;29:6058–6065. [PubMed: 2200519]
11. Finlin BS, Shao H, Kadono-Okuda K, Guo N, Andres DA. Rem2, a new member of the Rem/Rad/Gem/Kir family of Ras-related GTPases. Biochem J 2000;347 (Pt 1):223–231. [PubMed: 10727423]
12. Ward Y, Spinelli B, Quon MJ, Chen H, Ikeda SR, Kelly K. Phosphorylation of critical serine residues in Gem separates cytoskeletal reorganization from down-regulation of calcium channel activity. Mol Cell Biol 2004;24:651–661. [PubMed: 14701738]
13. Beguin P, et al. Regulation of Ca^{2+} channel expression at the cell surface by the small G-protein kir/Gem. Nature 2001;411:701–706. [PubMed: 11395774]
14. Nicholls A, Sharp KA, Honig B. Protein folding and association: insights from the interfacial and thermodynamic properties of hydrocarbons. Proteins 1991;11:281–296. [PubMed: 1758883]
15. Sprang SR. G protein mechanisms: insights from structural analysis. Annu Rev Biochem 1997;66:639–678. [PubMed: 9242920]

Abbreviations

RT
: room temperature

RGK
: Rad,Gem/Kir

VDCC
: voltage-dependent calcium channel

CaM

calmodulin

AP
: alkaline phosphatase

GMPPNP
: β, γ-imido-GTP

WT
: wild type

Appendix A. Supplementary data

Crystallographic coordinates and structure factors have been deposited in the PDB (2HT6).

Supplementary data associated with this article can be found, in the online version, at doi: 10.1016/j.febslet.2006.09.067.

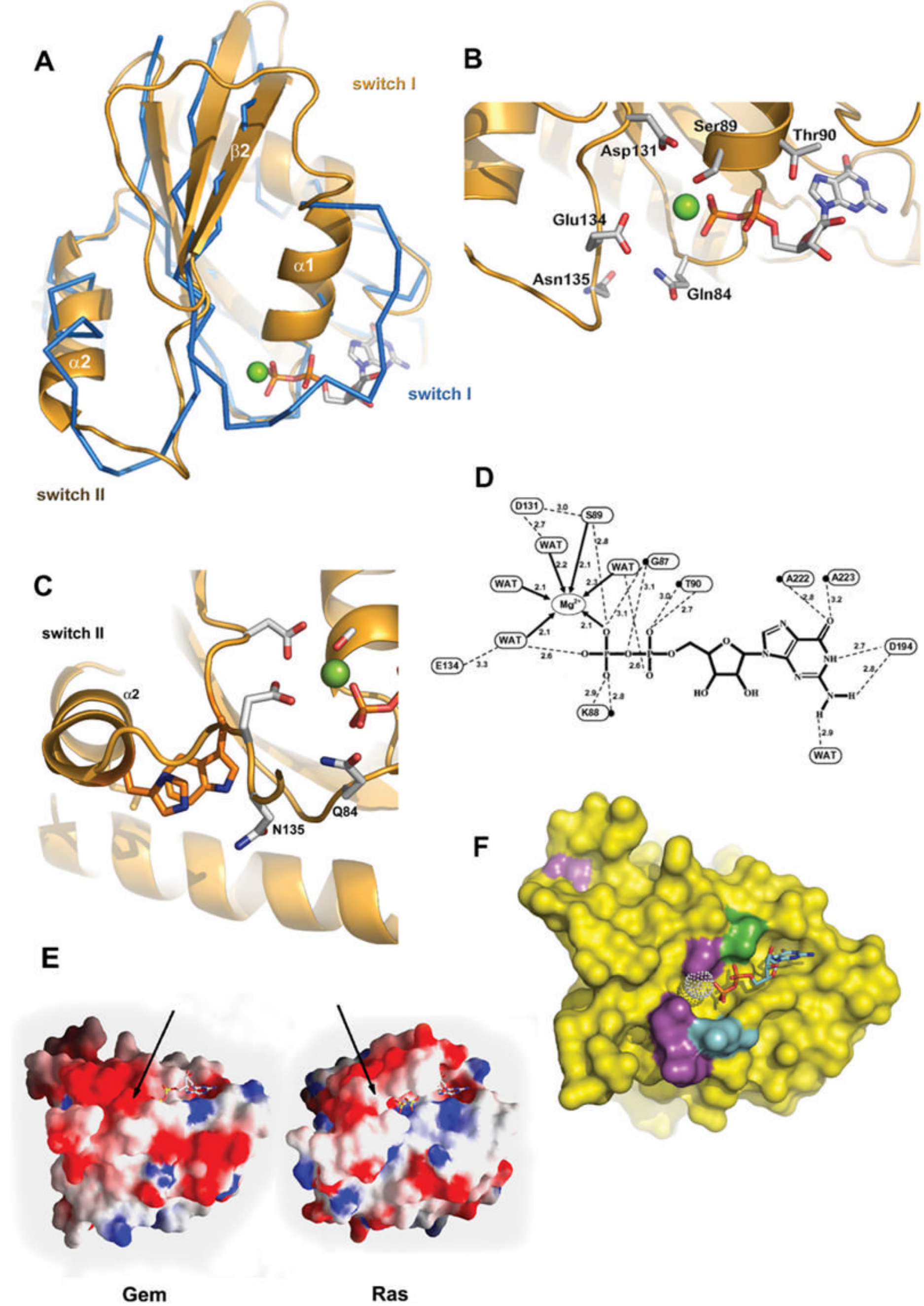

Fig 1.

Gem G-domain crystal structure. (A). Ribbon depiction of the Gem G-domain, colored in gold, with the superimposed Ras-GDP structure (PDB 4Q21) shown in blue. (B). Close-up of the Gem nucleotide binding region with interacting side chains drawn. Orientation is the same as A. (C). Depiction of switch II with its molecular linchpin, the stacking of H143 on W133. (D). Schematic representation of nucleotide interactions. Thick arrows denote the Mg^{2+} coordination shell, dashed lines represent H-bonds with side chains or waters, while a filled circle attached to a residue indicates the amide main chain of that residue. Distances are listed in Å. (E). Gem and Ras electrostatic potentials projected onto their respective molecular surfaces. The potential was calculated at 0.1 M ionic strength without nucleotide using Grasp

[14]. The arrows indicate approximately where the γ-phosphate would lie. (F). Molecular surface of Gem G-domain with bound GDP. Residues colored in magenta diminish VDCC β association, those in cyan perturb cytoskeletal remodeling, and that in green perturb both. The Mg^{2+} is drawn as a dotted sphere with a stick representation of GDP. Since β association may be GTP-dependent [13], this depiction may not accurately represent the relevant Gem conformation. Figure prepared with PyMOL.

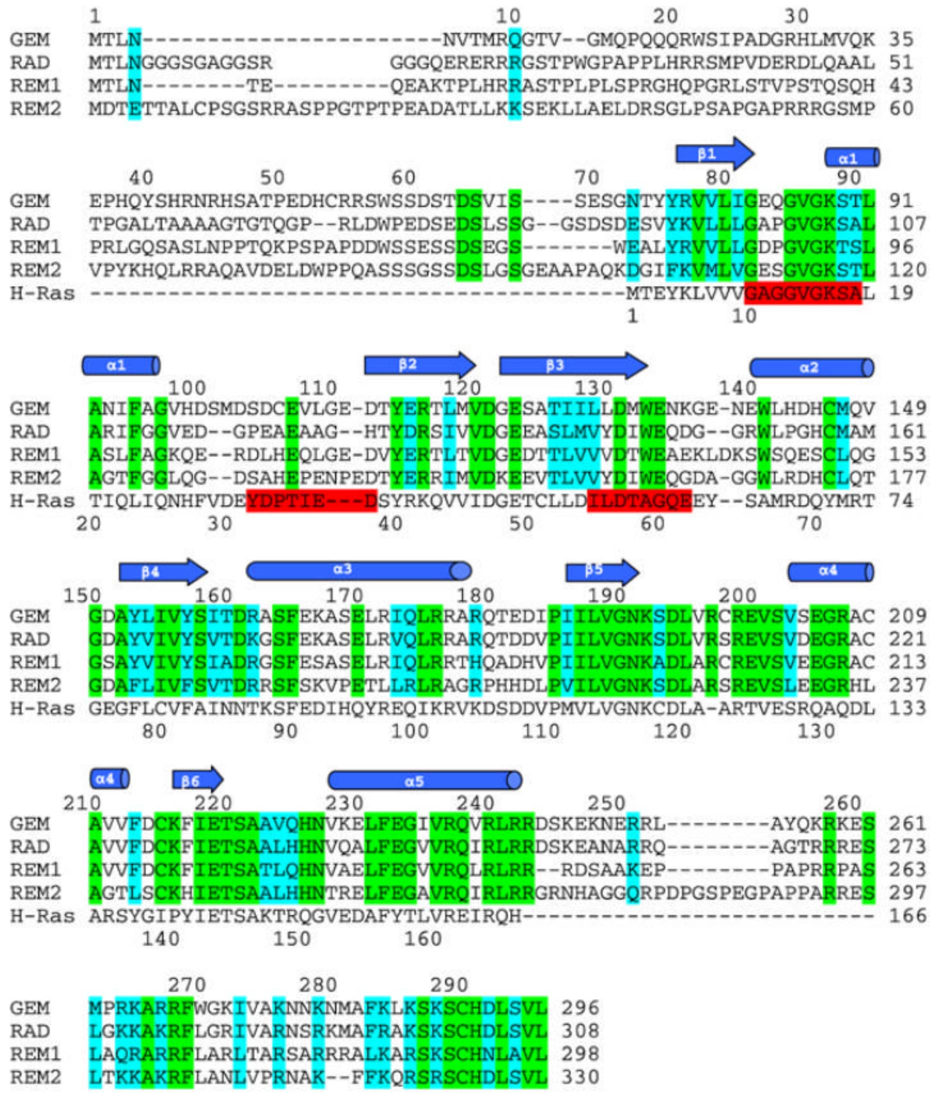

Fig 2.
Sequence alignment and structural features of Gem. Sequences of the RGK members human Gem (SwissProt P55040), human Rad (P55042), human Rem1 (O75628), and human Rem2 were aligned using CLUSTALW. Structure-based sequence alignment was performed with H-Ras (PDB 5P21). Gem residue numbering appears above the aligned sequences, whereas the H-Ras numbering appears below. Secondary structure elements were assigned with DSSP, where arrows denote beta strands and cylinders denote alpha helices. Absolute conservation amongst RGK proteins is highlighted in green while conservative substitution is highlighted by cyan. Ras sequences highlighted in red are the G1, G2, and G3 regions of H-Ras as described by Sprang [15].

NIH-PA Author Manuscript
NIH-PA Author Manuscript

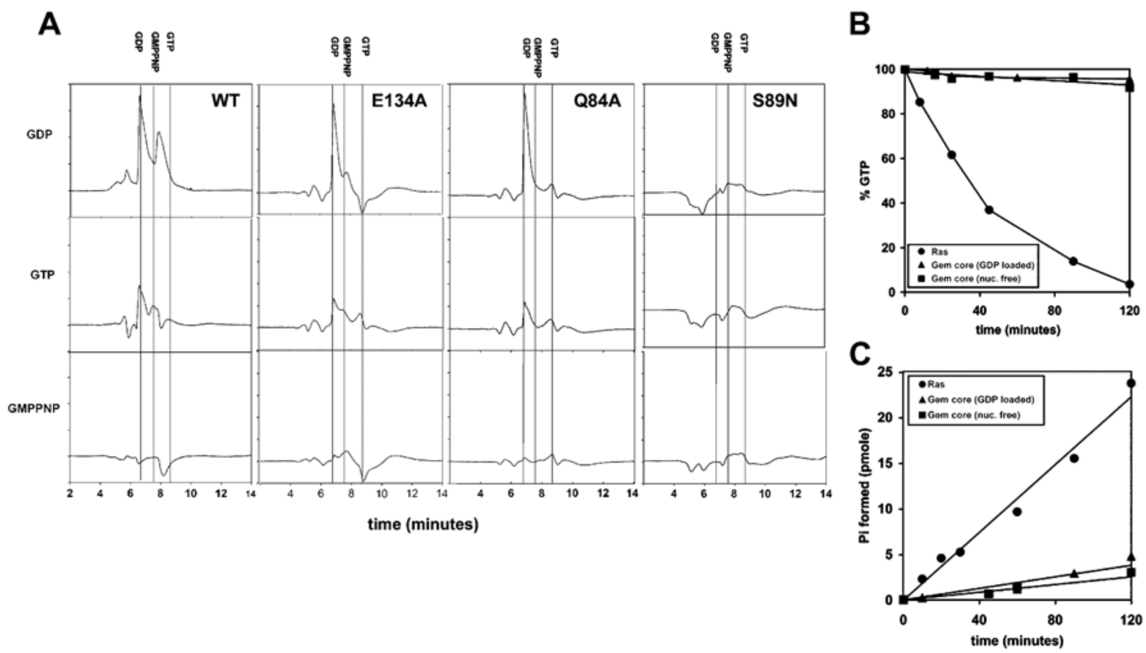

Fig 3.
Reversed-phase HPLC identification of bound nucleotides in WT Gem G-domain and mutants. (A) All panels show elution profiles under isocratic conditions where the abscissa is elution time and the ordinate is absorbance (252 nm). Nucleotide elution time standards are denoted for GDP, GTP, and GMPPNHP. Top, middle, and bottom panels show empty WT Gem or mutants incubated with GDP, GTP, or GMPPNHP, respectively, and processed as described in the results. Equimolar quantities were loaded on the column for all experiments. (B) and (C) Single-turnover and steady-state GTP hydrolysis assays, respectively. Gem G-domain, loaded with GDP or empty (nucleotide free) are drawn as filled triangles and squares, respectively while Ras, which served as the positive control is drawn as filled circles.

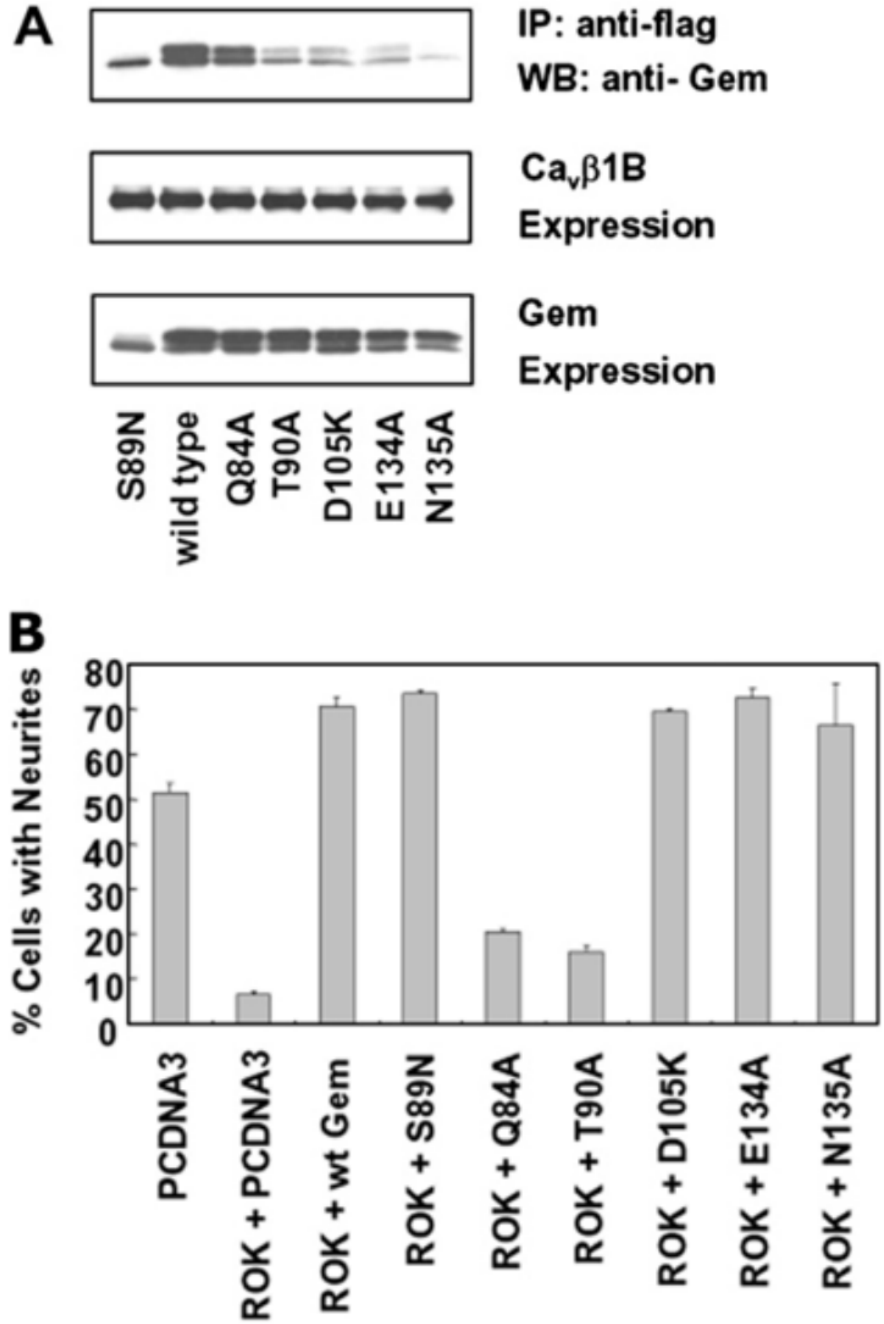

Fig 4.

Functional effects of Gem G-domain mutations. (A) Cos7 cells were co-transfected with plasmids encoding WT or mutant forms of Gem and flag-tagged Cavβ2A or Cavβ1B. A Western blot for Gem bound to immunoprecipitated Cavβ1B is shown. Mutation of residues possibly involved in Gem nucleotide binding (S89N, T90A, E134A, N135A) and D105K result in varying diminished interaction with Ca$_v$β1B. Gem Q84A demonstrated WT-like interaction with β. Cavβ2A produced similar results. (B) N1E-115 neuroblastoma cells were co-transfected with vectors encoding EGFP, ROK, and WT or mutant forms of Gem. In the presence of ROK, GFP-positive cells are predominantly round. WT Gem opposes ROK activity and leads to cell flattening and neurite extensions. In contrast to the Ca$_v$β interaction studies, E134A, N135A, and D105K strongly oppose ROK function in cytoskeletal restructuring like WT, while Q84A and T90A are inactive in this ROK-dependent assay. Results are expressed as the mean of three independent experimental results ± S.E.M.

Table 1

Crystallographic statistics

	Native	SeMet
Data statistics		
Wavelength (Å)	1.541	0.9788
Space group	$P2_12_12_1$	$P2_12_12_1$
Unit cell parameters (Å)	a = 39.5; b = 81.0; c = 124.1	a = 39.8; b = 81.4; c = 124.1
Total reflections	71678	232164
Unique reflections	12177	16469
Completeness (%)[a]	99.9 (99.9)	99.8 (100)
R_{merge} (%)[a,b]	6.9 (38.7)	7.3 (28.2)
I/σ[a]	12.1 (4.4)	21.8 (9.2)
Resolution range (Å)	50–2.65	50–2.4
f''	–	8.6
Phasing power (anomalous)	–	0.751
Figure of merit	–	0.17
X-ray source	Rigaku rotating anode	ESRF beamline ID14-4
Refinement statistics		
Number of reflections (working/test)	14724/830	
d_{min} (Å)	2.4	
R_{work}/R_{free}(%)	22.6/28.7	
Rms deviation from ideality		
Bond lengths	0.011	
Bond angles	1.407	
B factors (Å^2) (rmsd of bonded atoms-main/side chain)	1.7/2.7	
Average B factor (Å ^{2})	42.8	
Number of protein–ligand atoms/solvent	2677/86	

[a]Values of the highest resolution shell are given in parentheses.

[b]$R_{merge} = S_{hkl}S_i|I_{hkl,\,i} - \langle I \rangle_{hkl}|/S_{hkl}S_i|I_{hkl,\,i}|$ where I_{hkl} is the intensity of a reflection and $\langle I \rangle_{hkl}$ is the average of all observations of this reflection.